

# Investigation of spontaneous ordering in GaInP using reflectance difference spectroscopy

J. S. Luo, J. M. Olson, and K. A. Bertness  
National Renewable Energy Laboratory, Golden, Colorado 80401

M. E. Raikh and E. V. Tsiper  
University of Utah, Salt Lake City, Utah 84112

(Received 25 January 1994; accepted 19 April 1994)

Reflectance difference spectroscopy (RDS) is applied to the study of optical anisotropy in spontaneously ordered GaInP grown by metalorganic chemical-vapor deposition. The degree of ordering in GaInP has been associated previously with a shift of the band-gap energy  $\Delta E_0$ , and a crystal-field valence-band splitting  $\Delta_C$ . Theoretically and experimentally, both quantities are approximately proportional to the square of the order parameter, which varies from 0 to 1 for disordered and perfectly ordered GaInP, respectively. In this study, we examined a number of GaInP layers grown under conditions that yield a wide range of band-gap energies. The main spectral feature in all samples is a bulk-related, asymmetric peak at  $E_0$  with a long tail that extends well below  $E_0$  and a sharp, high-energy cutoff at  $E_0 + \Delta_C$ . The intensity of this peak is proportional to  $\sqrt{\Delta E_0}$  and is therefore linear with the order parameter. By annealing GaInP in  $\text{PH}_3/\text{H}_2$  mixtures, we find that the RD spectral features for energies between  $E_0 + \Delta_C$  and 3 eV are mainly surface induced. Evidence for a bulk-related RDS peak at  $E_1$  is also found.

## I. INTRODUCTION

Spontaneous atomic-scale ordering in  $\text{Ga}_{0.52}\text{In}_{0.48}\text{P}$  (hereafter referred to as GaInP) grown by metal-organic chemical-vapor deposition (MOCVD) has attracted considerable attention in recent years.<sup>1-5</sup> The degree of ordering is defined such that for  $\eta=1$ , the completely ordered GaInP is composed of alternating  $\{111\}$  planes of GaP and InP. For  $\eta<1$ , the alternating planes are composed of  $\text{Ga}_{0.5+\eta/2}\text{In}_{0.5-\eta/2}\text{P}$  and  $\text{Ga}_{0.5-\eta/2}\text{In}_{0.5+\eta/2}\text{P}$ . Associated with the ordering are two major electronic features: (1) the band gap  $E_0$  is reduced by more than 100 meV,<sup>6,7</sup> and (2) at the  $\Gamma$  point, the valence-band maximum, which is fourfold degenerate in disordered GaInP, is split with an energy difference  $\Delta_C$ .<sup>2</sup> Theoretically, the ordering-induced shift of the band gap<sup>8,9</sup> ( $\Delta E_0$ ) and  $\Delta_C$ <sup>9</sup> are related to the degree of ordering in GaInP. In previous work, photoluminescence (PL),<sup>2,10,11</sup> photoluminescence excitation (PLE),<sup>10-12</sup> and piezomodulated reflectance (PZR)<sup>13,14</sup> were used to measure  $\Delta E_0$  and  $\Delta_C$ . Experimentally,<sup>13</sup> it is found that  $\Delta_C$  is effectively proportional to  $\Delta E_0$ , which implies that, to first order, both are proportional to  $\eta^2$ . Therefore, for samples with weak ordering ( $\eta<0.2$ ), observation of the ordering in GaInP becomes very difficult. The maximum observed  $\Delta_C$  (at 15 K) is 31 meV for ordered GaInP with  $E_0=1.88$  eV ( $\Delta E_0=0.12$  eV).<sup>13</sup>

In this article, we use reflectance difference spectroscopy (RDS) to examine GaInP epilayers grown under conditions that yield a wide range of band-gap energies. RDS measures the anisotropy of optical reflectance, and heretofore, was used to study the anisotropic surface reconstruction of III-V materials with isotropic bulk properties.<sup>15</sup> For ordered GaInP, bulk anisotropic electronic<sup>16</sup> and optical properties<sup>2,10-14</sup> were observed previously. So we expect RDS to measure both the surface and bulk anisotropic optical features of GaInP. In the following sections, we show that the main spectral feature in all MOCVD-grown samples is a bulk-

related, asymmetric peak at  $E_0$  with a high-energy tail that includes  $\Delta_C$  and a peak intensity that varies with  $\sqrt{\Delta E_0}$ . This means that the RDS peak intensity at  $E_0$  is linear with  $\eta$ , which makes RDS particularly useful for detecting small degrees of ordering in GaInP. We also calculate the RDS line shape and intensity of an ordered alloy using the Luttinger model.<sup>17</sup> The calculation represents well the main RD spectral feature at  $E_0$ . Additional experiments show that the strong RD spectral features at energies greater than  $E_0$  are surface related.

## II. EXPERIMENTAL DETAILS

A schematic of the *in situ* RDS/MOCVD setup is shown in Fig. 1. A detailed description of the RDS technique can be found in the work of Aspnes *et al.*<sup>15</sup> In this study, RDS measures the difference between the reflectance of light polarized along  $[1\bar{1}0]$  and  $[110]$ . The incident light is *S* polarized and parallel to the  $[010]$  direction of the sample. The angle of incidence is  $11\pm1^\circ$  for the *ex situ* measurements and less than  $5^\circ$  for the *in situ* setup. To eliminate base line artifacts due to optical component anisotropy, we first measure  $(R_{1\bar{1}0} - R_{110} + \Delta R_B)$  and then rotate the sample by  $90^\circ$  and measure  $(R_{110} - R_{1\bar{1}0} + \Delta R_B)$ , where  $R_{1\bar{1}0}$  and  $R_{110}$  are reflectance of the light polarized along  $[1\bar{1}0]$  and  $[110]$ , respectively, and  $\Delta R_B$  is the base line. One half the difference of these two measurements eliminates  $\Delta R_B$ . This procedure also checks the reproducibility of the measured spectra, which is particularly important for small RDS signals. To eliminate the contribution to the baseline of wobble during the sample-stage rotation, a He-Ne laser is used to monitor and reposition the sample if necessary. The setup is capable of correcting sample tilt with a precision of 1 arcmin. We find that the base line of the RD spectrum changes by less than  $1.0\times10^{-3}$  if the tilt is less than 2 arcmin. The sensitivity of our RDS system is about  $1\times10^{-3}$ .

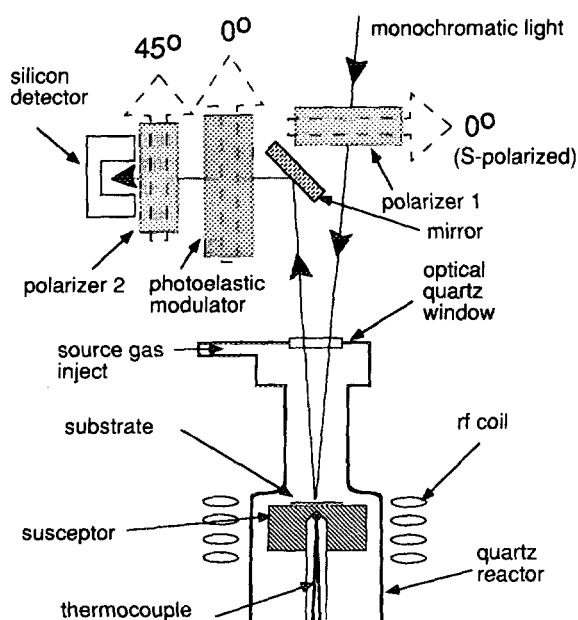


FIG. 1. Schematic arrangement of the *in situ* RDS/MOCVD experimental setup.

For *in situ* measurements, we use the apparatus shown in Fig. 1 to measure the RD spectrum of a sample at a given temperature and in an atmosphere other than air (e.g.,  $N_2$ ,  $H_2$ , or  $H_2+PH_3$ ).

All *ex situ* RDS measurements are performed in air at room temperature with no special sample preparation performed before the measurement. Most of the samples have been stored in the air for periods of days to months. Immersing the samples in a 10% HCl:H<sub>2</sub>O solution for 5 min before a measurement has virtually no effect on the RD spectrum of a given sample, and the spectrum of a freshly grown sample is essentially the same as that for the sample after "aging."

Most of the samples were grown by atmospheric-pressure MOCVD using various growth conditions to effect changes in the degree of order and optical properties of the alloy.<sup>18</sup> The general growth information for the MOCVD samples can be found elsewhere.<sup>18</sup> For comparison, we also examined a single GaInP sample grown by liquid-phase epitaxy (LPE). This sample has a "normal" band gap of 1.92 eV at room temperature and exhibits no evidence of ordering.

All samples were grown on vicinal (001) GaAs substrates. The degree of ordering and the optical properties of GaInP are also functions of the substrate tilt or misorientation from the (001) plane.<sup>10,11,19</sup> The amount of substrate tilt is noted for each sample with  $X^\circ B$  indicating a misorientation of  $X^\circ$  from the (001) plane toward the (111)*B* plane.

### III. RESULTS

In Fig. 2 we compare the RD intensity [measured as  $2(R_{1\bar{1}0}-R_{110})/(R_{1\bar{1}0}+R_{110})$ ] as a function of photon energy for samples representative of moderately ordered (low  $E_0$ ), weakly ordered, and disordered (high, "normal"  $E_0$ ) GaInP. The existence (or absence) of ordering has been verified by

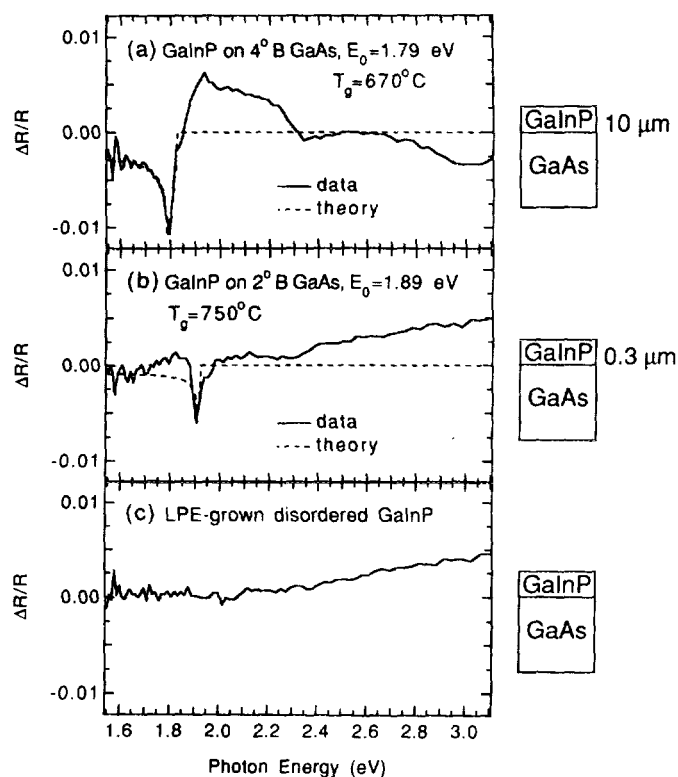


FIG. 2. RD spectra for (a) low band-gap ( $E_0=1.79$  eV) GaInP, (b) weakly ordered, high band-gap ( $E_0=1.90$  eV) GaInP, and (c) LPE-grown, disordered high band-gap GaInP.

other techniques, such as transmission electron diffraction. We observe at least four spectral signatures for the most ordered GaInP samples, but only one for the disordered samples. For the most ordered sample [Fig. 2(a)], the four features include (1) a sharp, negative, and asymmetrical peak at the band-gap energy, (2) a broad and positive spectral feature extending from approximately  $E_0$  to 2.2 eV, (3) a negative, but very small peak at around 2.35 eV, and (4) a negative, broad peak at around 3.0 eV. For the disordered, LPE-grown sample [Fig. 2(c)], the sharp peak near the band gap (1.92 eV) is absent. The only clear feature in the RD spectrum of the disordered sample is a very broad peak that begins around 2.2 eV and supposedly peaks somewhere beyond the spectral range of the RD instrument. This feature is presumably from the surface, and, interestingly, is also seen in the weakly ordered sample [Fig. 2(b)]. Below 2.1 eV, the RD spectrum of the weakly ordered sample also shows features similar to that of the most ordered sample—most notably, a sharp, negative peak near  $E_0$ .

It is reasonable to expect that the peak RDS intensity at  $E_0$ ,  $(\Delta R/R)_{E_0}$ , varies with the degree of order in the GaInP. Because  $\Delta E_0$  is basically proportional to  $\eta^2$ ,<sup>8,9</sup> the relation between  $(\Delta R/R)_{E_0}$  and  $\eta$  can be explored by plotting  $(\Delta R/R)_{E_0}$  as a function of  $\Delta E_0$ , where  $\Delta E_0$  is obtained by subtracting the measured band-gap energy from 1.92 eV (the room-temperature band-gap energy for disordered GaInP). Doing so for a series of samples, we find that  $(\Delta R/R)_{E_0}$  is approximately linear with  $\sqrt{\Delta E_0}$  (or  $\eta$ ), as shown in Fig. 3(a). This result is particularly important when  $\eta$  in GaInP is

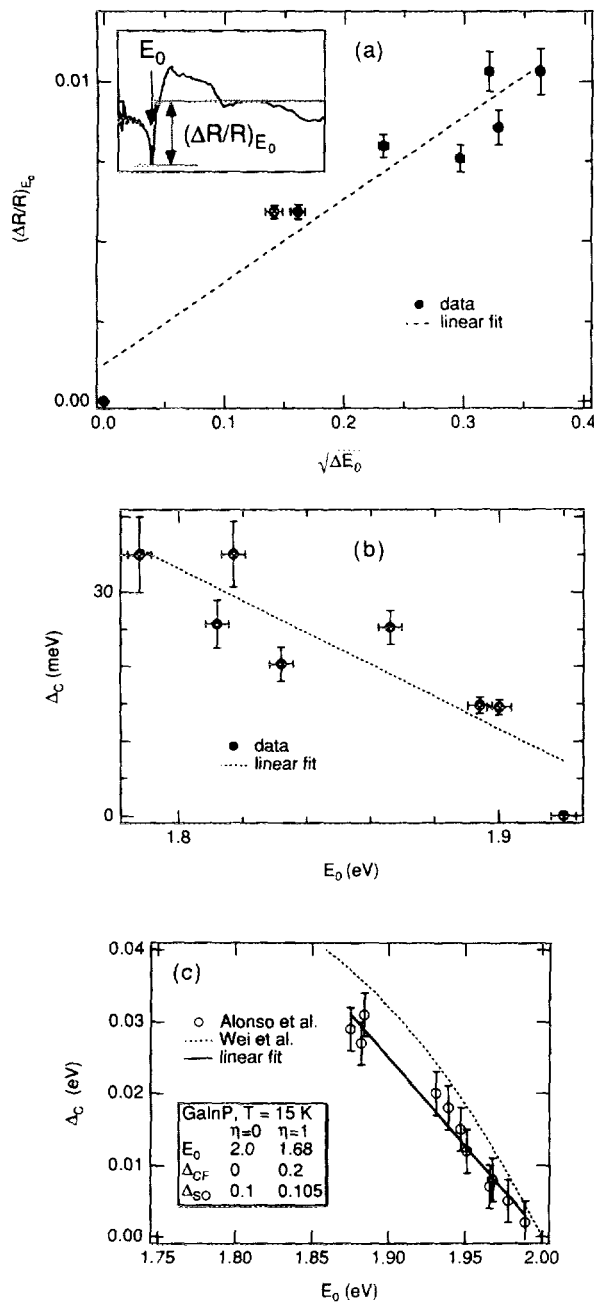


FIG. 3. (a) Plot of RDS intensity at  $E_0$  vs  $\sqrt{\Delta E_0}$ . Solid dots are measured data and dashed line is a linear fit to the data. (b) and (c) are plots of  $\Delta_C$  vs  $E_0$ . In (b)  $\Delta_C$  is estimated from fits to RD line shapes for a series of GaInP samples with a range of band gaps. Dots are estimated data and the dashed line is a linear fit to the data. In (c)  $\Delta_C$  vs  $E_0$  measured at 15 K by Alonso *et al.* (Ref. 13) using piezomodulated photoreflectance compared with theory of Wei *et al.* (Ref. 9) using the parameters specified in the box. The value of  $E_0$  for disordered GaInP is taken from Liedenbaum *et al.* (Ref. 26) and DeLong *et al.* (Ref. 27). The relationship between the term  $\Delta_C$  used in this article and the term  $\Delta_{CF}$  used by Wei *et al.* (Ref. 3) is  $\Delta_C \approx (\frac{2}{3})\eta^2\Delta_{CF}$  for  $\eta \ll 1$  and  $\Delta_C \approx \Delta_{SO}$ .

small. As mentioned previously, when  $\eta^2 \ll 1$ , the magnitudes of  $\Delta E_0$  and  $\Delta_C$ , which are both proportional to  $\eta^2$ , become comparable to the measurement uncertainty. Such is the case for the sample of Fig. 2(b): experimentally  $\Delta E_0 = 20 \pm 10$  meV and theoretically,  $\Delta_C = 8 \pm 4$  meV,<sup>9</sup> yet we measure a

very clear signal which is distinctively different from the spectrum of the disordered LPE sample.

## IV. DISCUSSION

### A. Theory

In this section, we calculate the reflectance difference for the light polarized along  $[110]$  and  $[1\bar{1}0]$  as a function of energy for a material exhibiting an anisotropic splitting  $\Delta_C$  of the valence-band maximum. The reflectance of light with polarization  $\alpha$  can be expressed in terms of the refraction coefficient  $n_\alpha$  and the extinction coefficient  $k_\alpha$  as

$$R_\alpha = \frac{(n_\alpha - 1)^2 + k_\alpha^2}{(n_\alpha + 1)^2 + k_\alpha^2}. \quad (1)$$

The calculation of reflectance as a function of photon energy requires information about the anisotropic valence-band structures and the corresponding wave functions, which are then used for calculating  $k_\alpha$

$$k_\alpha(\omega) = \frac{2\pi^2 e^2}{m_0^2 n_0 \omega^2} \sum_{\mu \mathbf{K}} |M_{\mu \mathbf{K}}^\alpha|^2 \delta[\hbar \omega - (E_{\mathbf{K}}^c - E_{\mu \mathbf{K}}^\nu)]. \quad (2)$$

Here  $\omega$  is the frequency of light;  $E_{\mathbf{K}}^c$  and  $E_{\mu \mathbf{K}}^\nu$  are energies of the conduction and valence bands;  $m_0$  is the free-electron mass;  $n_0$  is the refraction index in the absence of ordering; index  $\mu = \{l_1, l_2, h_1, h_2\}$  numerates two pairs, “l” as light holes and “h” as heavy holes, of the valence bands; and  $M_{\mu \mathbf{K}}^\alpha$  is the matrix element for the momentum operator projected along  $\alpha$ ,  $P_\alpha = -i\hbar \partial/\partial x_\alpha$ , taken between the wave functions of the conduction and valence bands. Note that the branches of the valence bands are degenerate in pairs:  $E_{h_1 \mathbf{K}}^\nu = E_{h_2 \mathbf{K}}^\nu$  and  $E_{l_1 \mathbf{K}}^\nu = E_{l_2 \mathbf{K}}^\nu$ . From Eq. (2), using the Kramers–Kronig relations and the Luttinger model,<sup>17</sup> the extinction and refraction coefficients are<sup>20</sup>

$$k_\alpha(\omega) = \frac{\beta}{(\hbar \omega)^2} \left( \frac{4}{3} \sqrt{\hbar \omega - E_0 - \Delta_C} + \sin^2 \theta_\alpha (\sqrt{\hbar \omega - E_0} - \sqrt{\hbar \omega - E_0 - \Delta_C}) \right), \quad (3)$$

$$n_\alpha(\omega) = n_0 - \frac{\beta}{(\hbar \omega)^2} \left( \frac{4}{3} \sqrt{E_0 + \Delta_C - \hbar \omega} + \sin^2 \theta_\alpha (\sqrt{E_0 - \hbar \omega} - \sqrt{E_0 + \Delta_C - \hbar \omega}) \right), \quad (4)$$

where  $\beta = [e^2(2m^*)^{3/2}/2\hbar m_0^2 n_0] p_{cv}^2$ ,  $p_{cv}$  is the Kane matrix element, and  $\theta_\alpha$  is the angle between the polarization of light and the ordering axis. The effective mass  $m^*$  is defined<sup>20</sup> as

$$m^* = \left[ \frac{1}{2} \left( \frac{m_e m_l}{m_e + m_l} \right)^{3/2} + \frac{1}{2} \left( \frac{m_e m_h}{m_e + m_h} \right)^{3/2} \right]^{2/3}, \quad (5)$$

where  $m_e$ ,  $m_l$ , and  $m_h$  are masses of the electron, light hole, and heavy hole, respectively. Here, we also use the convention that each of the square roots in Eqs. (3) and (4) is assumed to be zero when the argument is negative.

TABLE I. Values of parameters in Eq. (7) and (8) used to fit the RDS peak at  $E_0$  of GaInP.

Sample	$c$ [(eV) <sup>-3/2</sup> ]	$E_0$ (fit) <sup>a</sup> (eV)	$\Delta_C$ (meV)	$E_0^b$ (eV)
K316	0.18 <sup>c</sup>	1.791	35±5	1.788
K783	0.18	1.825	26±3	1.812
K303	0.18	1.786	35±4	1.817
TR20	0.18	1.820	20±2	1.832
K865	0.18	1.879	25±2	1.866
TR21	0.18	1.895	15±1	1.894
K078	0.18	1.909	15±1	1.900
	0.16 <sup>d</sup>			

<sup>a</sup>The RDS peak position used for the fit.  
<sup>b</sup>Band-gap energy measured by photoelectrochemical spectral response and corrected for lattice mismatch (Ref. 24). This energy is also used in the plot of  $\Delta_C$  vs  $E_0$  [Fig. 3(b)] and in calculating  $\Delta E_0$ .  
<sup>c</sup>This is the value of  $c$  that yielded the best line-shape fit for sample K316. For the other samples,  $c$  is fixed at this value;  $E_0$ (fit) is varied to fit the peak energy; and  $\Delta_C$  is varied to fit the peak intensity.  
<sup>d</sup>Calculated from the theoretical expression derived in Sec. IV A using  $n_0=3.5$ ,  $m^*\approx m_e/2=0.04 m_0$ , and  $[P_{CV}^2/(2m_0)]=20$  eV (Ref. 25).

For any realistic values of parameters, we should have  $|n(\omega) - n_0| \ll n_0$ . Then the differential of Eq. (1) can be simplified to

$$\Delta R(\omega) \approx 4 \frac{(n_0 - 1) \Delta n(\omega)}{(n_0 + 1)^3}, \tag{6}$$

where  $\Delta n(\omega) = n_{1\bar{1}0} - n_{110}$ . In deriving Eq. (6), we neglected terms proportional to  $k^2(\omega)$  because  $k(\omega)$  is in the order of  $|n(\omega) - n_0|$ .

The values of  $\sin^2 \theta_\alpha$  between the ordering axis  $[1\bar{1}1]$  and each of the directions  $[110]$ ,  $[1\bar{1}0]$  are 1 and  $\frac{1}{3}$ , respectively. With Eqs. (4) and (6), we then obtain the RDS intensity as a function of photon energy

$$\frac{\Delta R}{R} = - \frac{c}{(\hbar\omega)^2} (\sqrt{\Delta_C + E_0 - \hbar\omega} - \sqrt{E_0 - \hbar\omega}). \tag{7}$$

Here  $c = 8\beta/3(n_0^2 - 1)$ .

Equations (6) and (7) account for most of the bulk physical effects described in the previous section. Using Eq. (7), the RDS peak occurs at  $\hbar\omega = E_0$  and is given by

$$\left(\frac{\Delta R}{R}\right)_{E_0} = - \frac{c}{E_0^2} \sqrt{\Delta_C}. \tag{8}$$

Because  $\Delta_C$  is proportional to  $\Delta E_0$ , Eq. (8) is equivalent to the experimental result of Fig. 3(a).

The *ex situ* RDS spectra of a number of GaInP samples with various band-gap energies were fitted with Eq. (7), using  $c$ ,  $E_0$ , and  $\Delta_C$  as fitting parameters. The fitting data are shown in Table I. The fitted value of  $c$  (0.18 eV<sup>-3/2</sup>) is within 10% of the calculated value of  $c$  (0.16 eV<sup>-3/2</sup>). The line shape of samples K316 and K078 is shown as a dashed line in Figs. 2(a) and 2(b), respectively.

For low band-gap samples similar to K316, the fit is very good. The fitted values of  $\Delta_C$  (see Table I) are comparable to those measured by PZR,<sup>13</sup> and the line shape reproduces the pronounced subband-gap tail observed in the RD spectra. This tail is “predicted” by Eq. (6), which shows that the bulk

RDS signal in the vicinity of  $E_0$  is sensitive to  $\Delta n(\omega) = n_{1\bar{1}0} - n_{110}$  as opposed to  $\Delta k(\omega)$ . This is also consistent with the interference oscillations observed for samples of intermediate thicknesses.<sup>20</sup>

For high band-gap samples similar to K078, which are presumably less ordered, the line-shape fit is not as good, particularly for energies less than  $E_0$ . Also, the fitted value of  $\Delta_C = 15$  meV is about a factor of five larger than that measured by PZR.<sup>13</sup> These discrepancies are not understood at this time.

A plot of  $\Delta_C$  versus  $E_0$  using the data from Table I is shown in Fig. 3(b). A similar plot, constructed from PZR measurements<sup>13</sup> taken at  $T = 15$  K, is shown in Fig. 3(c). Although there is more scatter in the RDS data, both plots exhibit an essentially linear variation of  $\Delta_C$  with  $E_0$ . This supports our original assumption that  $\eta$  is small. Also, if  $\eta$  were close to 1, one expects to observe a polarized interband transition between the spin-orbit band and the conduction band with an energy of  $E_0 + \Delta_S$ . However, no polarization dependence of this transition has been observed by Alonso *et al.*<sup>13</sup> or Kanata *et al.*<sup>21</sup> Although this transition is shown<sup>13</sup> to blueshift slightly (relative to  $E_0$ ) for low band-gap GaInP, the shift rate,  $\partial\Delta_S/\partial E_0$ , is a factor of two lower than that predicted by theory.<sup>9</sup> This suggests that the crystal-field/spin-orbit coupling and  $\eta$  are small. This also implies that  $\Delta E_0(\eta=1)$  is larger than that calculated by Wei and Zunger (0.32 eV)<sup>22</sup> or Capaz and Koiller (0.13 eV).<sup>8</sup> These results are supported by preliminary transmission electron-diffraction results which indicate that  $\eta < 0.4$  for a sample grown under conditions similar to those of the sample of Fig. 2(a). If these diffraction data are correct, then it implies that  $\Delta E_0(\eta=1) > 0.75$  eV.

B. Surface-induced RDS features in GaInP

The peak at  $E_0$  is caused by an ordering-induced splitting of the valence-band maximum—a bulk property. In Fig. 2, we noted at least three other spectral features of ordered GaInP (the positive plateau just beyond  $E_0$ , and negative “peaks” at 2.35 and 3.0 eV), and it is tempting to ascribe these also to bulk ordering-induced transitions.<sup>20</sup> However, we have found that the spectral intensity for  $E > E_0 + \Delta_C$  is strongly modulated by changes in the GaInP surface. To confirm this point, we performed an experiment designed to modify exclusively the surface (or near surface) of GaInP. The results are shown in Fig. 4. Curve (1) in Fig. 4 is the initial RDS spectrum of a partially ordered GaInP sample. This spectrum was measured at  $T = 85^\circ\text{C}$  *in situ*, two days after the growth of this sample. During that two days it was stored *in situ* under a purge gas of supposedly oxygen-free  $\text{N}_2$  and had not been exposed to air. Nevertheless, the spectrum is virtually identical to that of the air-exposed sample of Fig. 2(a). Curve (2) in Fig. 4 is the RDS spectrum of the same sample measured *in situ* at  $T = 180^\circ\text{C}$  in an atmosphere of 1 mol %  $\text{PH}_3$  in  $\text{H}_2$ . This measurement was then repeated at 300, 400  $^\circ\text{C}$ , etc. The time at each temperature was 20 min or less. Curve (7) was measured at  $T = 85^\circ\text{C}$  in  $\text{H}_2$  immediately after cooling from sequence step (6). By analogy with GaAs, we assume that annealing GaInP in the presence of  $\text{H}_2$  and  $\text{PH}_3$ , above some temperature, removes any oxides from

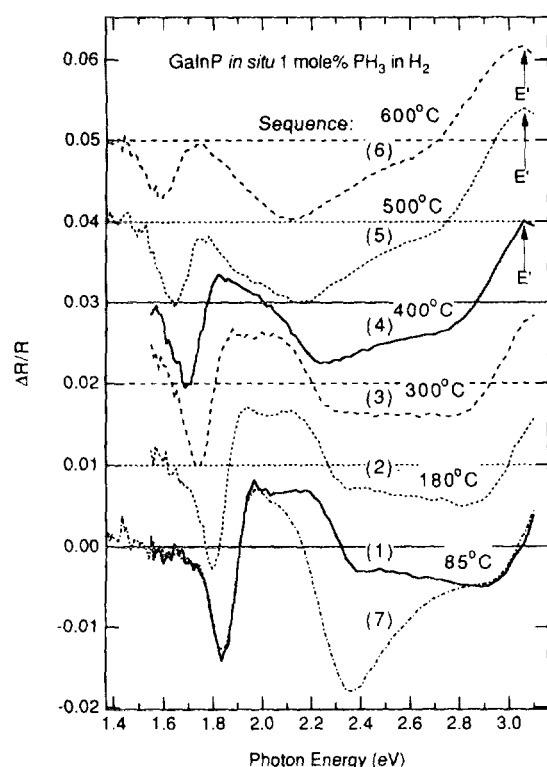


FIG. 4. Effect of  $\text{PH}_3$  annealing on RD spectra of GaInP measured *in situ* in 1 mol %  $\text{PH}_3$  in  $\text{H}_2$ .

the surface and yields a P-stabilized (presumably, dimerized) surface. Comparing the spectra of sequence steps (1) and (7), we see clearly that the peak at 2.35 eV and part of the positive plateau are definitely surface related. From this and other experiments, we also find that (i) the 2.35 eV peak can be quenched by exposing the surface to air at room temperature or annealing the sample in  $\text{H}_2$  (with no  $\text{PH}_3$ ) at 400 °C, (ii) the annealing rate in  $\text{H}_2$  or  $\text{PH}_3/\text{H}_2$  mixtures is slow (on the time scale of tens of minutes) at temperatures around 300 °C, and (iii) the 2.35 eV peak persists unaltered for temperatures between 400 and 600 °C and  $\text{PH}_3$  mole fractions between 0.1% and 2%. Note also that the peak shift with temperature for the  $E_0$  and 2.35 eV peaks are virtually identical.

The peaks at 1.85 eV ( $E_0$ ) and the low-energy side of the plateau are essentially unchanged, and one therefore might conclude that they are both bulk related. However, the positive peak on the low-energy side of plateau disappears (reversibly) at high temperature, suggesting that it too may be a surface peak.

Curves (4), (5), and (6) give a different picture of the 3.0 eV "peak." As the annealing (and measurement) temperature is increased, we see a peak, which we label  $E'$ , redshift to energies less than 3.1 eV. This suggests that the 3.0 eV "peak" at 85 °C is simply an inflection between the 2.35 eV surface peak and  $E'$ . At low temperatures, despite the fact that only the tail of  $E'$  is visible, we can see that it appears to be unaffected by the condition of the surface, implying that it is bulk induced.  $E'$  is probably related to the  $E_1$  peak of GaInP reported by Kurtz, Olson, and Kibbler using

electroreflectance.<sup>23</sup> They showed that the position of  $E_1$  varies with ordering from about 3.25 to 3.3 eV but did not investigate the polarization dependence of this transition. Further study of these observations is needed.

## V. CONCLUSIONS

We have demonstrated that RDS is a useful nondestructive technique for studying ordering in GaInP. The main spectral feature in all samples is a bulk-induced, asymmetric peak at  $E_0$  with a long tail that extends well below  $E_0$  and a sharp, high-energy cutoff at  $E_0 + \Delta_C$ . We find that the intensity of this peak is proportional to  $\sqrt{\Delta E_0}$  and is therefore linear with  $\eta$ . This means that RDS should be particularly useful for measuring the optical anisotropy of weakly ordered ternary and quaternary alloys.

For energies between  $E_0 + \Delta_C$  and 3 eV, the RD spectrum of GaInP is mainly surface induced. A negative peak at 2.35 eV is dominant only in samples with P-stabilized surfaces that have not been exposed to air. Exposure of the GaInP surface to air at room temperature or  $\text{H}_2$  at 400 °C quenches the 2.35 eV peak and augments the high-energy side of a positive feature that extends from  $E_0 + \Delta_C$  to about 2.2 eV. From *in situ* RDS measurements at high temperature, we also find evidence for a bulk-related RDS peak at  $E_1$ .

## ACKNOWLEDGMENTS

The authors would like to thank Gary Giust for helping us set up the RDS system and Sverre Froyen for helpful conversations. We are also grateful to M. C. Wu, National Tsing Hua University, Hsinchu, Taiwan, for the LPE-grown GaInP sample. This work is supported by the U. S. Department of Energy, Office of Energy Research, Basic Energy Sciences.

- <sup>1</sup>M. Kondow, H. Kakibayashi, and S. Minagawa, *J. Cryst. Growth* **99**, 291 (1988).
- <sup>2</sup>A. Mascarenhas, S. Kurtz, A. Kibbler, and J. M. Olson, *Phys. Rev. Lett.* **63**, 2108 (1989).
- <sup>3</sup>S.-H. Wei and A. Zunger, *Appl. Phys. Lett.* **56**, 662 (1990).
- <sup>4</sup>T. Suzuki and A. Gomyo, *J. Cryst. Growth* **111**, 353 (1991).
- <sup>5</sup>S. Froyen, J. E. Bernard, R. Osorio, and A. Zunger, *Phys. Scr.* **T45**, 272 (1992).
- <sup>6</sup>M. C. DeLong, P. C. Taylor, and J. M. Olson, *Appl. Phys. Lett.* **57**, 620 (1990).
- <sup>7</sup>M. K. Lee, R. H. Horng, and L. C. Haung, *J. Cryst. Growth* **124**, 358 (1992).
- <sup>8</sup>R. B. Capaz and B. Koiller, *Phys. Rev. B* **47**, 4044 (1993).
- <sup>9</sup>S. H. Wei, D. B. Laks, and A. Zunger, *Appl. Phys. Lett.* **62**, 1937 (1993).
- <sup>10</sup>D. J. Mowbray, R. A. Hogg, M. S. Skolnick, M. C. DeLong, S. R. Kurtz, and J. M. Olson, *Phys. Rev. B* **46**, 7232 (1992).
- <sup>11</sup>M. C. DeLong, D. J. Mowbray, R. A. Hogg, M. S. Skolnick, M. Hopkinson, J. P. R. David, P. C. Taylor, S. R. Kurtz, and J. M. Olson, *J. Appl. Phys.* **73**, 5163 (1993).
- <sup>12</sup>G. S. Horner, A. Mascarenhas, S. Froyen, R. G. Alonso, K. Bertness, and J. M. Olson, *Phys. Rev. B* **47**, 4041 (1993).
- <sup>13</sup>R. G. Alonso, A. Mascarenhas, G. S. Horner, K. A. Bertness, S. R. Kurtz, and J. M. Olson, *Phys. Rev. B* **48**, 11833 (1993).
- <sup>14</sup>R. G. Alonso, A. Mascarenhas, S. Froyen, G. S. Horner, K. Bertness, and J. M. Olson, *Solid State Commun.* **85**, 1021 (1993).
- <sup>15</sup>D. E. Aspnes, J. P. Harbison, A. A. Studna, and L. T. Florez, *J. Vac. Sci. Technol. A* **6**, 1327 (1988).
- <sup>16</sup>D. J. Friedman, A. E. Kibbler, and J. M. Olson, *Appl. Phys. Lett.* **59**, 2998 (1991).

<sup>17</sup>J. M. Luttinger, Phys. Rev. **102**, 1030 (1956).

<sup>18</sup>S. R. Kurtz, J. M. Olson, and A. Kibbler, Appl. Phys. Lett. **57**, 1922 (1990).

<sup>19</sup>T. Suzuki and A. Gomyo, J. Cryst. Growth **99**, 60 (1990).

<sup>20</sup>J. S. Luo, J. M. Olson, S. R. Kurtz, D. Arent, K. A. Bertness, M. Raikh, and E. Tsiper (unpublished).

<sup>21</sup>T. Kanata, M. Nishimoto, H. Nakayama, and T. Nishino, Appl. Phys. Lett. **63**, 512 (1993).

<sup>22</sup>D. B. Laks, S. H. Wei, and A. Zunger, Phys. Rev. Lett. **69**, 3766 (1992).

<sup>23</sup>S. R. Kurtz, J. M. Olson, and A. Kibbler, Solar Cells **24**, 307 (1988).

<sup>24</sup>S. R. Kurtz and J. M. Olson, *Rapid Characterization of Photovoltaic Materials Using Photoelectrochemical Techniques* (IEEE, New Orleans, LA, 1987), p. 823.

<sup>25</sup>Landolt-Bornstein, *Numerical Data and Functional Relationships in Science and Technology* (Springer, Berlin, 1982).

<sup>26</sup>C. T. H. F. Liedenbaum, A. Valster, A. L. G. J. Severens, and G. W. Thooft, Appl. Phys. Lett. **57**, 2698 (1990).

<sup>27</sup>M. C. DeLong, D. J. Mowbray, R. A. Hogg, M. S. Skolnick, J. E. Williams, S. R. Kurtz, J. M. Olson, M. C. Wu, and M. Hopkinson (unpublished).